J Nanopart Res (2015) 17:165
DOI 10.1007/s11051-015-2972-y

RESEARCH PAPER

Facilitated transport of titanium dioxide nanoparticles by humic substances in saturated porous media under acidic conditions

Ruichang Zhang · Haibo Zhang · Chen Tu · Xuefeng Hu · Lianzhen Li · Yongming Luo · Peter Christie

Received: 15 December 2014 / Accepted: 18 March 2015 / Published online: 1 April 2015

Abstract The transport behavior of titanium dioxide nanoparticles (TiO_2 NPs, 30 nm in diameter) was studied in well-defined porous media composed of clean quartz sand over a range of solution chemistry under acidic conditions. Transport of TiO_2 NPs was dramatically enhanced by humic substances (HS) at acidic pH (4.0, 5.0 and 6.0), even at a low HS concentration of 0.5 mg L^{-1}. Facilitated transport of TiO_2 NPs was likely attributable to the increased stability of TiO_2 NPs and repulsive interaction between TiO_2 NPs and quartz sands due to the adsorbed HS. The mobility of TiO_2 NPs was also increased with increasing pH from 4.0 to 6.0. Although transport of TiO_2 NPs was insensitive to low ionic strength, it was significantly inhibited by high concentrations of NaCl and $CaCl_2$. In addition, calculated Derjaguin–Landau–Verwey–Overbeek (DLVO) interaction energy indicated that high energy barriers were responsible for the high mobility of TiO_2 NPs, while the secondary energy minimum could play an important role in the retention of TiO_2 NPs at 100 mmol L^{-1} NaCl. Straining and gravitational settlement of larger TiO_2 NPs aggregates at 1 mg L^{-1} HS, pH 5.0, and 2 mmol L^{-1} $CaCl_2$ could be responsible for the significant retention even in the presence of high energy barriers. Moreover, more favorable interaction between approaching TiO_2 NPs and TiO_2 NPs that had been already deposited on the collector resulted in a ripening-shape breakthrough curve at 2 mmol L^{-1} $CaCl_2$. Overall, a combination of mechanisms including DLVO-type force, straining, and physical filtration was involved in the retention of TiO_2 NPs over the range of solution chemistry examined in this study.

Keywords Titanium dioxide nanoparticles · Facilitated transport · Humic substances · Mechanisms · Aggregation · Straining · Transport phenomena

Electronic supplementary material The online version of this article (doi:10.1007/s11051-015-2972-y) contains supplementary material, which is available to authorized users.

R. Zhang · Y. Luo · P. Christie
Key Laboratory of Soil Environment and Pollution Remediation, Institute of Soil Science, Chinese Academy of Sciences, Nanjing 210008, China

R. Zhang
University of Chinese Academy of Sciences, Beijing, China

H. Zhang · C. Tu · X. Hu · L. Li · Y. Luo (✉)
Key Laboratory of Coastal Environmental Processes and Ecological Remediation, Yantai Institute of Coastal Zone Research, Chinese Academy of Sciences, Yantai 264003, China
e-mail: ymluo@yic.ac.cn

Introduction

Titanium dioxide nanoparticles (TiO_2 NPs) are one of the most extensively used types of metal oxide nanomaterials in a variety of commercial products

including cosmetics, coatings, paints, pigments, textiles, and photocatalysts (Chen and Mao 2007; Keller et al. 2013). Given that, TiO_2 NPs are inevitably released into the natural environment, especially in waste disposal sites or by accidental leakage events during manufacturing and transportation processes (Gottschalk et al. 2009; Lin et al. 2010). A modeling study showed that TiO_2 NPs were expected to have the highest concentrations out of engineered materials (TiO_2, ZnO, Ag, CNTs, and fullerenes) in all environmental compartments in the United States, Switzerland, and Europe (Gottschalk et al. 2009; Keller et al. 2013). In addition, a number of laboratory studies have noted adverse effects of TiO_2 NPs on organisms including animals (Menard et al. 2011), plants (Du et al. 2011), and microorganisms (Ge et al. 2011) in environmental media. And recent studies suggested that TO_2 NPs might facilitate the transport of coexisting pollutants in soils (Fang et al. 2011), and act as a carrier for Cd bioaccumulation in the ciliate *Tetrahymena thermophila* (Yang et al. 2014).

Once released into the environment, the potential exposure pathways and bioavailability of TiO_2 NPs will be strongly influenced by their stability and transport behaviors. Quantification of the mobility of engineered nanoparticles in hydrologic pathways from point of release to human or ecological receptors is therefore essential for assessing their environmental exposures (Bouchard et al. 2013). A substantial amount of work on transport and deposition behaviors of TiO_2 NPs has been conducted in various aqueous environmental conditions using well-controlled porous media packing columns. These investigations have provided insights into the influence of environmental conditions, such as pH, ionic strength, natural organic matter, and surfactants on the stability and mobility of TiO_2 NPs (Chen et al. 2011, 2012; Chowdhury et al. 2011; Fang et al. 2013; Shih et al. 2012; Solovitch et al. 2010; Wang et al. 2012). pH is a key factor affecting the electrokinetic properties and transport of TiO_2 NPs in porous media. The point of zero charge (PZC) of TiO_2 NPs usually falls within the range 4.4–6.2 (Chen et al. 2012; Dietrich et al. 2012; Loosli et al. 2013; Petosa et al. 2012), and the mobility of uncoated TiO_2 NPs would therefore be enhanced in alkaline conditions because of the unfavorable electrostatic repulsion between the particles and negatively charged collector (Fang et al. 2013; Solovitch et al. 2010; Wang et al. 2012). In contrast, when pH approached to the PZC, the concurrence of aggregation and limited mobility of bare TiO_2 NPs was observed in the porous media (Chowdhury et al. 2011; Godinez and Darnault 2011; Solovitch et al. 2010). pH of surface water and subsurface water is generally in the range of 5.0–9.0; however, some of environmental media in vast tropical and subtropical areas exist in acidic conditions. Despite the large number of publications on the aggregation and transport of TiO_2 NPs, there were very few systematic studies focusing on its stability and transport behavior under acidic conditions in porous media and few results available showed some discrepancy. The limited studies conducted showed inconsistent results, and both retention and mobility of TiO_2 NPs in porous media have been reported under acidic conditions. Fang et al. (2013) found that favorable attachment condition at pH 2.6 resulted in complete retention of TiO_2 NPs in both saturated and unsaturated porous columns. However, Chowdhury et al. (2011) demonstrated that a significant portion of TiO_2 NPs could be eluted from porous columns at pH 5.0, which might be attributed to the observed smaller aggregate size and blocking effect even with electrostatically favorable interaction between collector and TiO_2 NPs.

Natural organic matter (NOM) which is ubiquitously distributed in aquatic environments and soils is another key factor governing the environmental transport and fate of nanoparticles (Zhou et al. 2011). Adsorption of NOM onto the surface of TiO_2 NPs significantly altered the physicochemical characteristics and, as a result, affected their stability and mobility in aquatic media (Chen et al. 2012; Loosli et al. 2013; Petosa et al. 2012). The enhancement of stability and mobility of TiO_2 NPs in these studies was attributable to the electrostatic and/or steric repulsive effects of adsorbed NOM. Humic substances (HS) with abundant carboxylic (–COOH, –COO–) and phenolic (–OH) functional groups could exist as common negatively charged polyelectrolytes in aquatic environments (Jones and Su 2012). The presence of HS might inverse the positively charged TiO_2 NPs in acidic conditions, subsequently alter the favorable interaction between TiO_2 NPs and collector, and facilitate the mobility of the nanoparticles, thereby increasing the risk of TiO_2 NPs in acidic conditions.

The objective of this study was to investigate the influences of different environmentally relevant factors such as HS, pH, and ionic strength on the stability

and transport behavior of TiO_2 NPs in saturated porous media under acidic conditions. Systematic aggregation and mobility experiments of TiO_2 NPs, supplemented with necessary mechanisms governing the stability and transport, were performed. It was hoped that results of this study would provide insights into the potential fate and the subsequent risk of TiO_2 NPs in acidic environments.

Materials and methods

Characterization of the porous medium

Quartz sand (40–70 mesh) was obtained from Sinopharm Chemical Reagent Co., Ltd. The sand particles had an average diameter of approximately 350 μm. Surface impurities were removed by soaking in 12 mol L^{-1} HCl for 24 h followed by rinsing with deionized water (18.2 MΩ cm) until the pH of the rinse solution matched that of the deionized water. The media were then baked in a furnace (FB1400, Thermo Scientific) at 120 °C for 1 h and then at 800 °C for 5 h (Litton and Olson 1993).

Preparation of TiO_2 NPs suspensions

The TiO_2 NPs were obtained from Shanghai Aladdin Reagent Co., Ltd with a nominal size of 30 ± 10 nm and were used as received in all experiments. The crystalline composition of the nanoparticles was determined to be a pure anatase phase by X-ray diffraction (XRD, Ultima IV, Rigaku, Japan) (Fig. S1). The specific surface area of the nanoparticles was measured to be 80.8 m^2 g^{-1} in a multipoint mode using a TriStar II 3020 pore size and surface area analyzer. The PZC of TiO_2 NPs was determined to be 6.2 in deionized water (Fig. S2). Stocking suspension of TiO_2 NPs was prepared by adding 250 mg of nanoparticles to 1.0 L of deionized water. The suspension was sonicated for 30 min (500 W, 40 kHz) at room temperature (20 °C) and stored no longer than 2 days at 4 °C. Immediately prior to each experiment, an aqueous suspension containing a final TiO_2 NPs concentration of 50 mg L^{-1} and the desired solution chemistry was produced by diluting the stocking suspension in background solution. A wide range of background solution chemistry was examined in experiments, namely HS concentrations of 0–10 mg L^{-1}, pH 4.0–6.0, NaCl concentrations of 0.1–250 mmol L^{-1}, and $CaCl_2$ concentrations of 0.5–5.0 mmol L^{-1} (Table S2). The humic substances (fulvic acid ≥90 %, reported by the vendor) were supplied by Shanghai Aladdin Reagent Co., Ltd. and were used as a model NOM. Zeta potential and particle size distribution of the prepared TiO_2 NPs suspensions were measured with Zetasizer Nano ZS90 (Malvern Instruments).

Column experiments

Glass columns (2.5 cm in diameter and 10 cm in length) were packed uniformly with clean quartz sand. The resulting porosity of the porous medium was gravimetrically measured to be 0.42–0.47. Once packed, the column was flushed with at least 10 pore volumes (PV) of background solution with the desired HS, pH, and ions as a pre-equilibration procedure. Then 2 PV of TiO_2 NPs suspensions (50 mg L^{-1}) with the same background chemistry were introduced into the column, followed by a nanoparticle-free background electrolyte solution. The Darcy velocity was maintained at 0.35–0.38 cm min^{-1} for all experiments. Column effluent was collected using a BS-110A fraction collector (Huxi Analytical Instrument Factory Co., Ltd., China). The concentrations of TiO_2 NPs in the influent (C_0) and effluent (C) were determined spectrophotometrically at a wavelength of 343 nm. All transport experiments were conducted in duplicate with a deviation <3 %, and therefore, only one representative breakthrough curve for each experiment was shown in the results.

Results and discussion

Electrokinetic and aggregation properties of TiO_2 NPs in suspensions

The stability of nanoparticles in suspensions is a key factor affecting their transport and deposition behaviors in porous media (Espinasse et al. 2007). Experiments at pH 4.0 were conducted to quantify the modification of the surface charge and aggregation behavior of TiO_2 NPs by HS coating. As illustrated in Fig. 1a, a positive zeta potential of TiO_2 NPs was +28.4 mV in the absence of HS and declined to −3.6 mV at 0.5 mg L^{-1} of HS. A higher HS

concentration of 10 mg L^{-1} further depressed the zeta potential to −37.5 mV. As shown in Fig. S5, the amount of HS adsorbed onto TiO_2 NPs increased gradually from 0.109 mg m^{-2} under an initial HS concentration of 0.5 mg L^{-1}–0.833 mg m^{-2} under an initial HS concentration of 10 mg L^{-1} at pH 4.0. Adsorption of 0.109 mg m^{-2} HS on surfaces inversed the positive potential of TiO_2 NPs. The effect of HS on the zeta potential of TiO_2 NPs could be attributed to the negative charge of HS adsorbed onto the surface of TiO_2 NPs at the given pH (Fig. S2). Moreover, ligand exchange of hydroxyl groups on TiO_2 NPs surfaces with HS might diminish hydroxyl groups for protonation which could also be partly responsible for the decrease in the positive charge (Bian et al. 2011). Organic anions of HS (Table S1 and Fig. S4) could also increase the negative charge density adjacent to the particle surface and cause a shift in the position of the shear plane further away from the surface, and thus result in a decrease in zeta potential of TiO_2 NPs (Bian et al. 2011; Zhang et al. 2009). Because of the protonation of the surface groups of TiO_2 NPs and adsorbed HS, the zeta potential of TiO_2 NPs became less negative with decreasing pH from 6.0 to 4.0 (Fig. 1b). As shown in Fig. 1c, the absolute magnitude of the zeta potential of TiO_2 NPs varied inversely with ionic strength in aqueous solution with 5 mg L^{-1} HS at pH 5.0, due to the charge screen effect and electric double layer compression for all surfaces (Chen et al. 2012). In addition, binding of Ca^{2+} to the functional groups of HS coated on TiO_2 NPs could lead to a decrease of negative charge other than charge screening (Amirbahman and Olson 1995; Xu et al. 2011). These two mechanisms could explain the greater influence of $CaCl_2$ on the zeta potential of TiO_2 NPs than that of NaCl at the same ionic strength (Fig. 1d). Similar to previous reports (Chen et al. 2012), the surface of the quartz sand was negatively charged over the entire range of HS concentrations, pH, and ionic strength conditions examined in this study (Fig. 1).

Table 1 shows that all the TiO_2 NPs were present in aggregates larger than 400 nm rather than primary particles of 30 nm. DLVO patterns in Figs. 2 and S7 could interpret the aggregation of TiO_2 NPs. Net

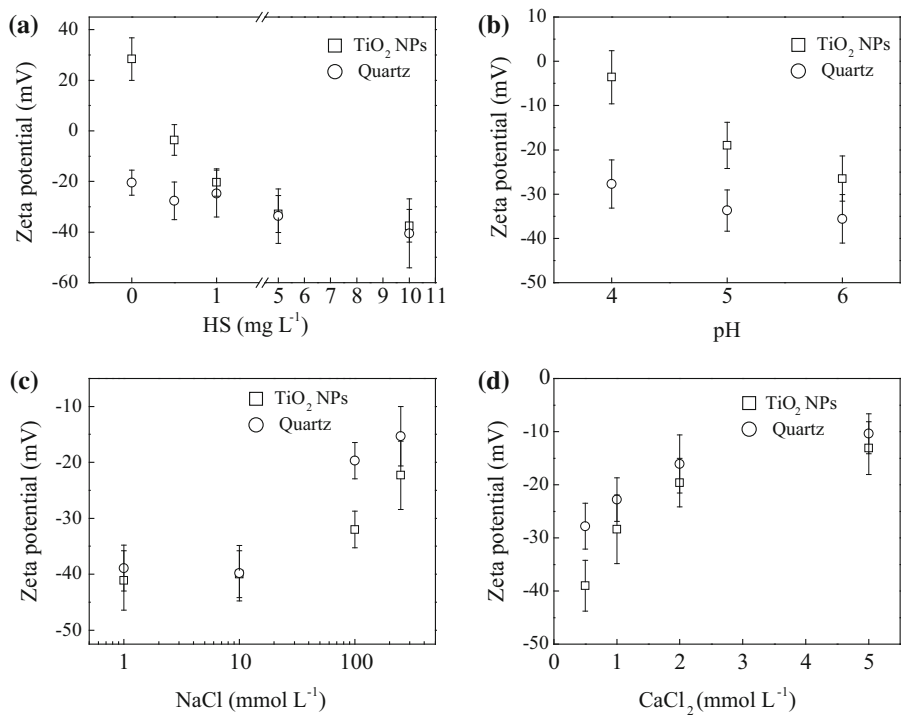

Fig. 1 Zeta potential of TiO_2 NPs and quartz as a function of HS concentration (pH 4.0 and 0.1 mmol L^{-1} NaCl) (**a**), pH (5 mg L^{-1} HS and 0.1 mmol L^{-1} NaCl) (**b**), NaCl concentration (pH 5.0 and 5 mg L^{-1} HS) (**c**), and $CaCl_2$ concentration (pH 5.0 and 5 mg L^{-1} HS) (**d**)

Table 1 Calculated filtration efficiencies for TiO_2 NPs with different HS concentrations, pH, NaCl, and $CaCl_2$ concentrations

Background condition		TiO_2 NPs size (d_p) (nm)	$C/C_{0\ max}$	Elution rate	Diffusion efficiency (η_D)	Interception efficiency (η_I)	Gravitation efficiency (η_G)	Total theoretical efficiency (η_0)	Removal efficiency (η)	Attachment efficiency (α)
HS	0 mg L^{-1}	665 ± 53	0	0	7.56×10^{-3}	1.02×10^{-5}	7.40×10^{-3}	1.50×10^{-2}		1
	0.5 mg L^{-1}	977 ± 82	0.20	0.20	5.90×10^{-3}	1.76×10^{-5}	1.59×10^{-2}	2.18×10^{-2}	6.5×10^{-3}	0.29
	1 mg L^{-1}	586 ± 34	0.74	0.65	8.05×10^{-3}	8.50×10^{-6}	5.77×10^{-3}	1.38×10^{-2}	1.9×10^{-3}	0.14
	5 mg L^{-1}	552 ± 26	0.85	0.88	8.27×10^{-3}	7.77×10^{-6}	4.85×10^{-3}	1.31×10^{-2}	0.55×10^{-3}	0.042
	10 mg L^{-1}	442 ± 27	0.88	0.95	1.10×10^{-2}	5.67×10^{-6}	3.20×10^{-3}	1.34×10^{-2}	0.22×10^{-3}	0.016
pH	4.0	977 ± 82	0.20	0.20	5.90×10^{-3}	1.76×10^{-5}	1.59×10^{-2}	2.18×10^{-2}	6.5×10^{-3}	0.29
	5.0	643 ± 49	0.68	0.69	7.77×10^{-3}	9.70×10^{-6}	6.93×10^{-3}	1.47×10^{-2}	1.6×10^{-3}	0.11
	6.0	529 ± 36	0.88	0.91	9.43×10^{-3}	7.34×10^{-6}	4.71×10^{-3}	1.41×10^{-2}	0.39×10^{-3}	0.027
NaCl	1 mmol L^{-1}	468 ± 39	0.90	0.92	1.01×10^{-2}	6.47×10^{-6}	3.95×10^{-3}	1.41×10^{-2}	0.34×10^{-3}	0.024
	10 mmol L^{-1}	484 ± 16	0.88	0.85	1.03×10^{-2}	5.65×10^{-6}	3.19×10^{-3}	1.35×10^{-2}	0.69×10^{-3}	0.051
	100 mmol L^{-1}	545 ± 43	0.38	0.38	9.39×10^{-3}	7.69×10^{-6}	5.16×10^{-3}	1.46×10^{-2}	4.0×10^{-3}	0.48
	250 mmol L^{-1}	705 ± 79	0	0	7.56×10^{-3}	1.09×10^{-5}	7.94×10^{-3}	1.55×10^{-2}		1
$CaCl_2$	0.5 mmol L^{-1}	497 ± 41	0.90	0.90	8.84×10^{-3}	7.65×10^{-6}	4.87×10^{-3}	1.37×10^{-2}	0.44×10^{-3}	0.031
	1 mmol L^{-1}	546 ± 36	0.87	0.89	8.25×10^{-3}	9.30×10^{-6}	6.38×10^{-3}	1.46×10^{-2}	0.46×10^{-3}	0.032
	2 mmol L^{-1}	794 ± 68	0.49	0.46	6.96×10^{-3}	1.31×10^{-5}	1.05×10^{-2}	1.75×10^{-2}	3.0×10^{-3}	0.17
	5 mmol L^{-1}	917 ± 103	0	0	5.75×10^{-3}	1.61×10^{-5}	1.40×10^{-2}	1.98×10^{-2}		1

The parameters were calculated on the basis of the representative breakthrough curves

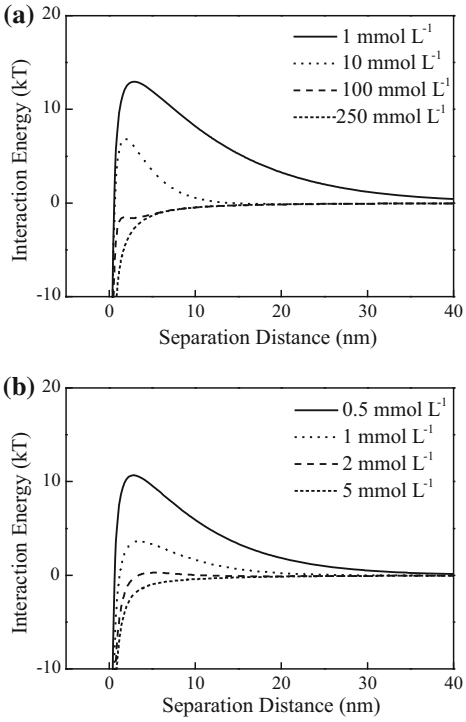

Fig. 2 Calculated DLVO interaction energy between TiO_2 NPs (based on primary size) under varying NaCl (**a**) and $CaCl_2$ (**b**) concentration (pH 5.0 and 5 mg L^{-1} HS)

repulsive energy barriers between TiO_2 NPs in all cases were <20 kT, the recognized limit for prevention of coagulation of particles after collision (Cosgrove 2005). Specially, electrostatically favorable conditions were observed in the background conditions of pH 4.0, 250 mmol L^{-1} NaCl, and 5 mmol L^{-1} $CaCl_2$. Deep primary energy wells in these cases resulted in aggregates of TiO_2 NPs larger than 700 nm. The details of interaction energy calculation are provided in the supplementary material.

As noted in Fig. S7, TiO_2 NPs had a net repulsive energy barrier in the absence of HS. With the addition of HS, the energy barrier decreased and approached zero at 0.5 mg L^{-1} HS, and this was observed visually by the greater size of 977 nm shown in Table 1. However, the net repulsive energy barrier began to increase with further addition of HS, a finding consistent with the decreasing of TiO_2 NPs aggregate size. Additionally, decreasing pH or elevating ionic strength resulted in reduction of the net repulsive barrier and then led to TiO_2 NPs aggregate of larger size. The diverse electrokinetic properties and aggregation of TiO_2 NPs would lead to a variety of mobility behaviors in porous media.

Transport of TiO_2 NPs in porous media under acidic conditions

The transport breakthrough curves of TiO_2 NPs were obtained for a wide range of solution chemistry, i.e., HS 0–10 mg L^{-1}, pH 4.0–6.0, NaCl 1–250 mmol L^{-1}, and $CaCl_2$ 0.5–5 mmol L^{-1}. Representative results of breakthrough curves are presented in Fig. 3 and Table 1. Pulse injection of TiO_2 NPs into columns yielded asymmetrical breakthrough curves that gradually rose to a maximum value before declining sharply to a relative concentration (C/C_0) approaching zero. Due to the opposite surface charges of quartz and nanoparticles, TiO_2 NPs were almost immobile in the absence of HS at the acidic pH tested (Fig. 3a, Fig. S9). Negative charge of both quartz sand and TiO_2 NPs resulting from the coating of HS on the surface indicated that the existence of electrostatic repulsive forces led to unfavorable conditions for deposition of TiO_2 NPs onto the collector (Chowdhury et al. 2011). The elution of TiO_2 NPs from the columns was dramatically enhanced with increase of HS, and the maximum C/C_0 observed increased from 0.20 to 0.88 with a change in HS concentration from 0.5 mg L^{-1} to 10 mg L^{-1} (Table 1). As noted from breakthrough curves of TiO_2 NPs with suspensions pH of 4.0, 5.0 and 6.0 (Fig. 3b), the pH was found to have significant effects on the transport of TiO_2 NPs. Increasing of $C/C_{0\,max}$ (Table 1) suggested that elevating pH from 4.0 to 6.0 facilitated the transport of TiO_2 NPs in the quartz sand columns. Results presented in Fig. 3c, d show the effect of NaCl and $CaCl_2$ on the mobility of TiO_2 NPs in porous media and almost similar transport behavior was observed with NaCl and $CaCl_2$ concentration <10 and <1 mmol L^{-1}, respectively. This suggested that the mobility of TiO_2 NPs was insensitive to low solution ionic strengths. However, the clear reduction of $C/C_{0\,max}$ demonstrated that mobility was observed at higher electrolyte concentrations, and this was consistent with the decrease of zeta potentials presented in Fig. 1. Furthermore, high ionic strengths such as 250 mmol L^{-1} NaCl or 5 mmol L^{-1} $CaCl_2$ led to deposition of all the TiO_2 NPs onto the porous media.

It is worth noting that NOM concentrations of groundwater and surface waters often fall in the ranges

from 0.25 to 5 and 2.5–50 mg L^{-1}, and can be up to around 2 g L^{-1} in wastewaters (Chen et al. 2012; Crittenden and Montgomery Watson Harza (Firm) 2005). Moreover, in ground water the concentrations of monovalent cations (e.g. Na^+, K^+) are typically 1–10 mmol L^{-1} and of divalent cations (e.g., Ca^{2+}, Mg^{2+}) are typically 0.1–2 mmol L^{-1} (Saleh et al. 2008). Therefore, according to results of the present study, it is reasonable to infer that TiO_2 NPs could be very stable and mobile in certain acidic surface waters and groundwater due to the abundance of NOM and relatively low ionic strength.

Mechanisms governing the transport of TiO_2 NPs

Interpretation with DLVO theory

Energy profiles for interactions between TiO_2 NPs and quartz sand across a range of solution conditions are presented in Figs. 4 and S9. High energy barrier (180–500 kT) existed between TiO_2 NPs and quartz sand with HS concentration >1 mg L^{-1} (Fig. S10a), suggesting unfavorable conditions for TiO_2 NPs retention in quartz sand columns. However, a substantial deep primary energy well (<−500 kT) occurred when HS concentration was <1 mg L^{-1}, indicating favorable conditions for TiO_2 NPs deposition onto quartz surfaces. The calculated interaction energy profiles were consistent with the observed mobility trends of TiO_2 NPs under different HS concentrations in the porous media columns. As indicated in previous studies, pH was another factor influencing the DLVO interaction energy (Fang et al. 2013). Higher pH (5.0 and 6.0) resulted in significant elution in column experiments due to high energy barrier (220–310 kT), whereas an electrostatically favorable condition observed at pH 4.0 induced marked retention of TiO_2 NPs in quartz (Fig. S10b).

According to electric double layer and DLVO theory, the higher the ionic strength, the lower the elution will be due to a low energy barrier and greater tendency for nanoparticle aggregation (He et al. 2008; Rahman et al. 2013). No energy barrier and deep primary energy well (<−800 kT) in DLVO profiles indicated completely favorable conditions for deposition of TiO_2 NPs onto surfaces of quartz in columns at 100 mmol L^{-1} NaCl (Fig. 4a) and 5 mmol L^{-1} $CaCl_2$ (Fig. 4b). Although a high energy barrier (34 kT) was observed for 100 mmol L^{-1} NaCl, the presence of the deep secondary energy well (−11 kT) could capture

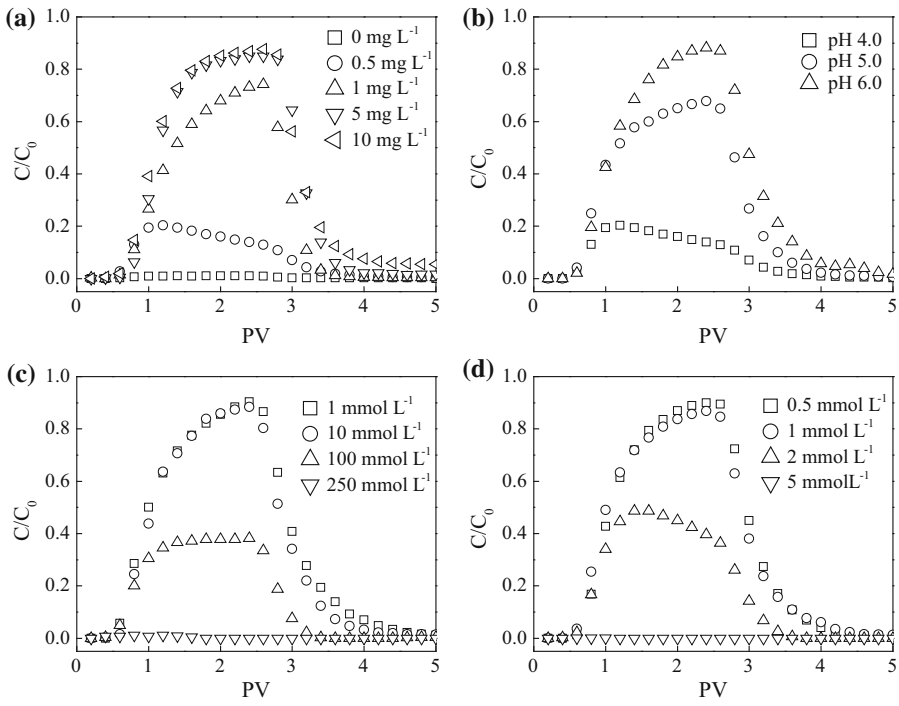

Fig. 3 Breakthrough curves for TiO_2 NPs at different HS concentrations (**a**), pH (**b**), NaCl concentrations (**c**), and $CaCl_2$ concentrations (**d**)

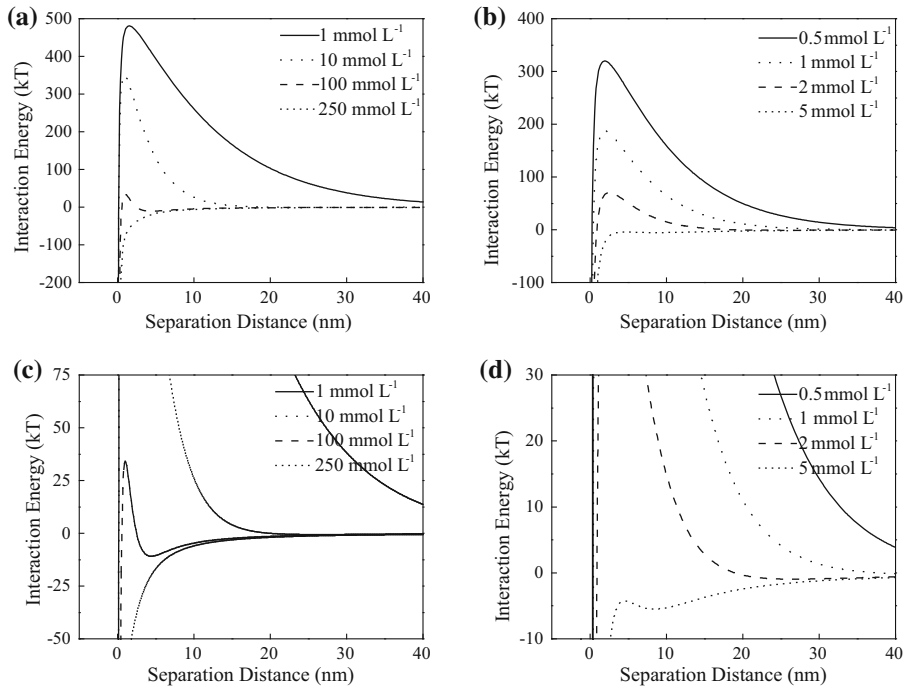

Fig. 4 Calculated DLVO interaction energy between TiO_2 NPs (based on aggregated size) and quartz sand under varying NaCl (**a**, **c**) and $CaCl_2$ (**b**, **d**) concentration (pH 5.0 and 5 mg L^{-1} HS)

substantial TiO_2 NPs unless they had sufficient kinetic energy to escape back into solution. Given this, 72 % of TiO_2 NPs in the influent deposited in the column.

Surprisingly, a high energy barrier for 2 mmol L^{-1} $CaCl_2$ (70 kT), as well as for pH 5.0 (220 kT) and 1 mg L^{-1} HS (180 kT), did not prevent TiO_2 NPs from depositing onto surfaces of quartz as anticipated. Hence, some of the observed transport trends were inconsistent with the DLVO predictions, and this might be explained by aggregation and subsequent straining (Chowdhury et al. 2011; Rahman et al. 2013; Solovitch et al. 2010).

Contribution of TiO_2 NPs aggregation and straining

DLVO theory predicts only particle–particle and particle–collector interactions, but it is insufficient for the description of physicochemical processes including straining, ripening, and blocking (Chowdhury et al. 2011; Elimelech 1995). Blocking is referred to as a continuous decrease of the rate of particle deposition due to the non-availability of attachment sites on the surface of the collector grains (Song and Elimelech 1993). The phenomenon is most important under conditions of favorable particle–collector interaction and unfavorable particle–particle interaction (Chowdhury et al. 2011; Song and Elimelech 1993). However, since favorable particle–collector interaction and unfavorable particle–particle interaction did not occur simultaneously, blocking might not have occurred in this study. The aggregation of TiO_2 NPs, common in all tested conditions, and subsequent straining might contribute to the retention of particles in packed columns with background solution of 2 mmol L^{-1} $CaCl_2$, pH 5.0, and 1 mg L^{-1} HS, in spite of the presence of energy barriers >70 kT.

Straining is the trapping of colloid particles in the downgradient pore throats that are too small to allow particle passage (Mcdowellboyer et al. 1986). In principle, straining is controlled by the size of the nanoparticles and the pore size distribution characteristics of porous media. Empirically, straining has been considered to be an important particle retention mechanism when the ratio of the colloid diameter to the mean gain diameter is greater than 0.0017 (Bradford et al. 2002; Chen et al. 2012). Since the average size of quartz packed in columns in this study was 350 μm, the threshold of nanoparticle aggregates size for straining would be 595 nm. Due to insufficient repulsive energy between TiO_2 NPs, the size of

aggregates reached to 586, 643, 794 and 917 nm in background solution with 1 mg L^{-1} HS, pH 5.0, 2 mmol L^{-1} $CaCl_2$, and 0.5 mg L^{-1} HS, respectively. It is considerably inferred that straining under the latter three conditions would result in the significant retention of TiO_2 NPs in transport experiments. It is worth noting that, in hydrodynamic measurements, the size of aggregates in suspension at 1 mg L^{-1} HS was widely distributed (Fig. S11), and >30 % of aggregates exceeded the critical size of 595 nm. As a result, straining was inevitably involved in the retention of TiO_2 NPs under this condition. Although straining did not necessarily lead to ripening, the ripening-shape breakthrough curve in the study was obtained at 2 mmol L^{-1} $CaCl_2$ and 0.5 mg L^{-1} HS (Fig. 3), which illustrated the greater TiO_2 NPs mass transfer to collector surfaces. As shown in Fig. 5, no energy barrier existed between TiO_2 NPs, and a deeper energy well in the DLVO profile was calculated between TiO_2 NPs than that between TiO_2 NPs and quartz, which together could lead to more favorable interaction for attachment between approaching TiO_2 NPs and TiO_2 NPs that had already been deposited on the collector (Chen et al. 2011, 2012). Deposition of TiO_2 NPs was then enhanced, whereas it might be another factor responsible for the ripening phenomenon at 0.5 mg L^{-1} HS, that is, the larger TiO_2 NPs aggregates in this scenario blocked the path of the pores (Lu et al. 2013).

Physical filtration effect

Classic filtration theory is used to explain the mechanism for deposition of colloidal particles on

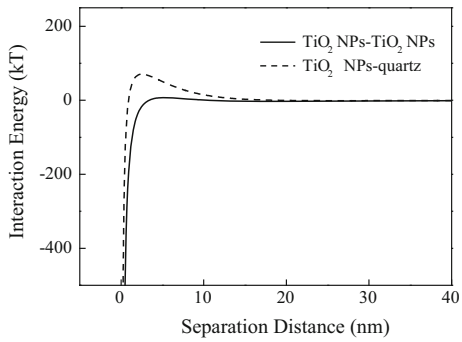

Fig. 5 Calculated DLVO interaction energy between TiO_2 NPs (based on aggregated size) and between TiO_2 NPs (based on aggregated size) and quartz sand at 2 mmol L^{-1} $CaCl_2$

porous media (Rahman et al. 2013; Tufenkji and Elimelech 2004; Yao et al. 1971). Particles suspended in pore fluid contact porous media surfaces through three mechanisms: diffusion, interception, and gravitational sedimentation. The efficiency of diffusion, interception, and gravitational sedimentation calculated for each background condition as provided in the supplementary material are listed in Table 1. In general, attachment efficiency (α) decreased with increasing of HS concentration and pH, and increased with increasing NaCl and $CaCl_2$ concentrations, which compared well with the elution rates in transport experiments. Values of $\alpha < 1$ were consistent with the significant mobility of TiO_2 NPs from porous media observed in experiments.

Diffusion efficiency (η_D) comprised 27–82 % of total filtration efficiency (η_0) under various conditions. It varied inversely with TiO_2 NPs size in the influent, which increased from 5.90×10^{-3} for 0.5 mg L^{-1} HS (TiO_2 NPs size of 977 nm) to 1.10×10^{-2} for 10 mg L^{-1} HS (TiO_2 NPs size of 442 nm). Numerous previous studies have reported diffusion as the predominant mechanism for deposition of nanoparticles <100 nm in porous media (He et al. 2009; Rahman et al. 2013; Zhuang et al. 2005). Due to the large aggregate size of TiO_2 NPs, gravitational sedimentation played an important role in this study. Contrary to η_D, gravitational efficiency (η_G) varied in the same direction as TiO_2 NPs size. Taking a batch of $CaCl_2$ as an example, η_G increased about three times for TiO_2 NPs in 5 mmol L^{-1} $CaCl_2$ (977 nm), compared with TiO_2 NPs in 0.5 mmol L^{-1} $CaCl_2$ (546 nm). Interception efficiency (η_I) was negligible relative to η_D and η_G, which comprised <1 % of total filtration efficiency (η_0) under various conditions. To sum up, diffusion was suggested to be a major mechanism for deposition of smaller TiO_2 NPs, while larger particles were retained primarily due to gravitational sedimentation.

Conclusions

The stability and transport behaviors of TiO_2 NPs in porous media columns packed with clean quartz were investigated in various background solutions under acidic conditions in the present study. Solution chemistry was found to have a remarkable effect on the electrokinetic properties and stability of TiO_2 NPs

and as a result on the mobility in the porous media. Due to the favorable interactions between TiO_2 NPs and the collector, TiO_2 NPs were immobile in the porous media at pH 4.0–6.0 in the absence of HS. Humic substances present in background solution were readily adsorbed onto the TiO_2 NPs surfaces and the adsorbed HS altered the electrokinetic properties of the TiO_2 NPs and quartz, and this drastically enhanced the stability and mobility of the TiO_2 NPs. Enhancement of mobility was also observed when the pH was elevated from 4.0 to 6.0. Although low ionic strength was unfavorable for TiO_2 NPs deposition and resulted in its high mobility in porous media, electrolyte concentrations >100 mmol L^{-1} NaCl or >2 mmol L^{-1} $CaCl_2$ significantly inhibited the mobility. DLVO theory together with straining and physical filtration effects could interpret the transport and retention of TiO_2 NPs in porous media well. High energy barriers facilitated the transport of TiO_2 NPs. However, the presence of secondary energy well, straining, and gravitational settlement of larger aggregates was the predominant mechanisms of deposition of TiO_2 NPs onto collector surfaces. This study suggested that in most acidic aquatic environment, NOM ubiquitously existing in natural waters could facilitate the mobility of TiO_2 NPs even in the presence of moderate ionic strength. The risk assessment of TiO_2 NPs in aquatic systems requires further study due to their high mobility.

Acknowledgments This work was supported by the National Natural Science Foundation of China (41171248, 41230858).

Conflict of interest The authors declare that they have no conflict of interest.

References

Amirbahman A, Olson TM (1995) Deposition kinetics of humic matter-coated hematite in porous-media in the presence of Ca^{2+}. Colloid Surf A 99:1–10. doi:10.1016/0927-7757(95)03134-Y

Bian SW, Mudunkotuwa IA, Rupasinghe T, Grassian VH (2011) Aggregation and dissolution of 4 nm ZnO nanoparticles in aqueous environments: influence of pH, ionic strength, size, and adsorption of humic acid. Langmuir 27:6059–6068. doi:10.1021/La200570n

Bouchard D, Zhang W, Chang XJ (2013) A rapid screening technique for estimating nanoparticle transport in porous media. Water Res 47:4086–4094. doi:10.1016/j.watres.2012.10.026

Bradford SA, Yates SR, Bettahar M, Simunek J (2002) Physical factors affecting the transport and fate of colloids in saturated porous media. Water Resour Res 38: 63-1-63-12 doi: 10.1029/2002wr001340

Chen X, Mao SS (2007) Titanium dioxide nanomaterials: synthesis, properties, modifications, and applications. Chem Rev 107:2891–2959. doi:10.1021/Cr0500535

Chen GX, Liu XY, Su CM (2011) Transport and retention of TiO_2 rutile nanoparticles in saturated porous media under low-ionic-strength conditions: measurements and mechanisms. Langmuir 27:5393–5402. doi:10.1021/La200251v

Chen GX, Liu XY, Su CM (2012) Distinct effects of humic acid on transport and retention of TiO_2 rutile nanoparticles in saturated sand columns. Environ Sci Technol 46:7142–7150. doi:10.1021/Es204010g

Chowdhury I, Hong Y, Honda RJ, Walker SL (2011) Mechanisms of TiO_2 nanoparticle transport in porous media: role of solution chemistry, nanoparticle concentration, and flowrate. J Colloid Interf Sci 360:548–555. doi:10.1016/j.jcis.2011.04.111

Cosgrove T (2005) Colloid science: principles, methods and applications. Blackwell Publishing, Oxford

Crittenden JC, Montgomery Watson Harza (Firm) (2005) Water treatment principles and design, 2nd edn. J. Wiley, Hoboken

Dietrich LAS, Sahu M, Biswas P, Fein JB (2012) Experimental study of TiO_2 nanoparticle adhesion to silica and Fe(III) oxide-coated silica surfaces. Chem Geol 332:148–156. doi:10.1016/j.chemgeo.2012.09.043

Du WC, Sun YY, Ji R, Zhu JG, Wu JC, Guo HY (2011) TiO_2 and ZnO nanoparticles negatively affect wheat growth and soil enzyme activities in agricultural soil. J Environ Monitor 13:822–828. doi:10.1039/C0em00611d

Elimelech M (1995) Particle deposition and aggregation: measurement, modelling, and simulation. Colloid and surface engineering series. Butterworth-Heinemann, Oxford

Espinasse B, Hotze EM, Wiesner MR (2007) Transport and retention of colloidal aggregates of C-60 in porous media: effects of organic macromolecules, ionic composition, and preparation method. Environ Sci Technol 41:7396–7402. doi:10.1021/Es0708767

Fang J, Shan XQ, Wen B, Lin JM, Owens G, Zhou SR (2011) Transport of copper as affected by titania nanoparticles in soil columns. Environ Pollut 159:1248–1256. doi:10.1016/j.envpol.2011.01.039

Fang J, Xu MJ, Wang DJ, Wen B, Han JY (2013) Modeling the transport of TiO_2 nanoparticle aggregates in saturated and unsaturated granular media: effects of ionic strength and pH. Water Res 47:1399–1408. doi:10.1016/j.watres.2012.12.005

Ge YG, Schimel JP, Holden PA (2011) Evidence for negative effects of TiO_2 and ZnO nanoparticles on soil bacterial communities. Environ Sci Technol 45:1659–1664. doi:10.1021/Es103040t

Godinez IG, Darnault CJG (2011) Aggregation and transport of nano-TiO_2 in saturated porous media: effects of pH, surfactants and flow velocity. Water Res 45:839–851. doi:10.1016/j.watres.2010.09.013

Gottschalk F, Sonderer T, Scholz RW, Nowack B (2009) Modeled environmental concentrations of engineered

nanomaterials (TiO_2, ZnO, Ag, CNT, fullerenes) for different regions. Environ Sci Technol 43:9216–9222. doi:10.1021/Es9015553

He YT, Wan JM, Tokunaga T (2008) Kinetic stability of hematite nanoparticles: the effect of particle sizes. J Nanopart Res 10:321–332. doi:10.1007/s11051-007-9255-1

He F, Zhang M, Qian TW, Zhao DY (2009) Transport of carboxymethyl cellulose stabilized iron nanoparticles in porous media: column experiments and modeling. J Colloid Interface Sci 334:96–102. doi:10.1016/j.jcis.2009.02.058

Jones EH, Su CM (2012) Fate and transport of elemental copper (Cu-0) nanoparticles through saturated porous media in the presence of organic materials. Water Res 46:2445–2456. doi:10.1016/j.watres.2012.02.022

Keller AA, McFerran S, Lazareva A, Suh S (2013) Global life cycle releases of engineered nanomaterials. J Nanopart Res 15:1–17. doi:10.1007/S11051-013-1692-4

Lin DH, Tian XL, Wu FC, Xing BS (2010) Fate and transport of engineered nanomaterials in the environment. J Environ Qual 39:1896–1908. doi:10.2134/Jeq2009.0423

Litton GM, Olson TM (1993) Colloid Deposition rates on silica bed media and artifacts related to collector surface preparation methods. Environ Sci Technol 27:185–193. doi:10.1021/Es00038a022

Loosli F, Le Coustumer P, Stoll S (2013) TiO_2 nanoparticles aggregation and disaggregation in presence of alginate and Suwannee River humic acids. pH and concentration effects on nanoparticle stability. Water Res 47:6052–6063. doi:10.1016/j.watres.2013.07.021

Lu YY, Xu XP, Yang K, Lin DH (2013) The effects of surfactants and solution chemistry on the transport of multiwalled carbon nanotubes in quartz sand-packed columns. Environ Pollut 182:269–277. doi:10.1016/j.envpol.2013.07.034

Mcdowellboyer LM, Hunt JR, Sitar N (1986) Particle-transport through porous-media. Water Resour Res 22:1901–1921. doi:10.1029/Wr022i013p01901

Menard A, Drobne D, Jemec A (2011) Ecotoxicity of nanosized TiO_2. Review of in vivo data. Environ Pollut 159:677–684. doi:10.1016/j.envpol.2010.11.027

Petosa AR, Brennan SJ, Rajput F, Tufenkji N (2012) Transport of two metal oxide nanoparticles in saturated granular porous media: role of water chemistry and particle coating. Water Res 46:1273–1285. doi:10.1016/j.watres.2011.12.033

Rahman T, George J, Shipley HJ (2013) Transport of aluminum oxide nanoparticles in saturated sand: effects of ionic strength, flow rate, and nanoparticle concentration. Sci Total Environ 463:565–571. doi:10.1016/j.scitotenv.2013.06.049

Saleh N, Kim HJ, Phenrat T, Matyjaszewski K, Tilton RD, Lowry GV (2008) Ionic strength and composition affect the mobility of surface-modified Fe-0 nanoparticles in water-saturated sand columns. Environ Sci Technol 42:3349–3355. doi:10.1021/Es071936b

Shih YH, Liu WS, Su YF (2012) Aggregation of stabilized TiO_2 nanoparticle suspensions in the presence of inorganic ions. Environ Toxicol Chem 31:1693–1698. doi:10.1002/Etc.1898

Solovitch N, Labille J, Rose J, Chaurand P, Borschneck D, Wiesner MR, Bottero JY (2010) Concurrent aggregation and deposition of TiO_2 nanoparticles in a sandy porous media. Environ Sci Technol 44:4897–4902. doi:10.1021/Es1000819

Song L, Elimelech M (1993) Dynamics of colloid deposition in porous media: modeling the role of retained particles. Colloid Surf A 73:49–63. doi:10.1016/0927-7757(93)80006-Z

Tufenkji N, Elimelech M (2004) Correlation equation for predicting single-collector efficiency in physicochemical filtration in saturated porous media. Environ Sci Technol 38:529–536. doi:10.1021/Es034049r

Wang Y et al (2012) Transport of titanium dioxide nanoparticles in saturated porous media under various solution chemistry conditions. J Nanopart Res 14:1095. doi:10.1007/S11051-012-1095-Y

Xu YL, Qin Y, Palchoudhury S, Bao YP (2011) Water-soluble iron oxide nanoparticles with high stability and selective surface functionality. Langmuir 27:8990–8997. doi:10.1021/La201652h

Yang WW et al (2014) TiO_2 nanoparticles act as a carrier of Cd bioaccumulation in the ciliate *Tetrahymena thermophila*. Environ Sci Technol 48:7568–7575. doi:10.1021/Es500694t

Yao KM, Habibian MM, Omelia CR (1971) Water and waste water filtration: concepts and applications. Environ Sci Technol 5:1105–1112. doi:10.1021/Es60058a005

Zhang Y, Chen YS, Westerhoff P, Crittenden J (2009) Impact of natural organic matter and divalent cations on the stability of aqueous nanoparticles. Water Res 43:4249–4257. doi:10.1016/j.watres.2009.06.005

Zhou DM, Wang DJ, Cang L, Hao XZ, Chu LY (2011) Transport and re-entrainment of soil colloids in saturated packed column: effects of pH and ionic strength. J Soil Sediment 11:491–503. doi:10.1007/s11368-010-0331-2

Zhuang J, Qi J, Jin Y (2005) Retention and transport of amphiphilic colloids under unsaturated flow conditions: effect of particle size and surface property. Environ Sci Technol 39:7853–7859. doi:10.1021/Es050265j